

## **CRISPR/Cas9-mediated knockout of *Abcd1* and *Abcd2* genes in BV-2 cells: novel microglial models for X-linked Adrenoleukodystrophy**

Q. Raas<sup>a</sup>, C. Gondcaille<sup>a</sup>, Y. Hamon<sup>b</sup>, V. Leoni<sup>c</sup>, C. Caccia<sup>d</sup>, F. Ménétrier<sup>e</sup>, G. Lizard<sup>a,f</sup>, D. Trompier<sup>a</sup>, S. Savary<sup>a,\*</sup>

<sup>a</sup>Laboratoire Bio-PeroxiL EA7270, University of Bourgogne Franche-Comté, Dijon, France,

<sup>b</sup>Aix Marseille Univ, CNRS, INSERM, CIML, Centre d'Immunologie de Marseille-Luminy, Marseille, France,

<sup>c</sup>Laboratory of Clinical Chemistry, Hospital of Varese, ASST-Settelaghi, Milan, Italy,

<sup>d</sup>Laboratory of Medical Genetics and Neurogenetics, Foundation IRCCS Istituto Neurologico Carlo Besta, Milan, Italy,

<sup>e</sup>Centre des Sciences du Goût et de l'Alimentation, AgroSup Dijon, UMR6265/UMRA1324, CNRS, INRA, University of Bourgogne Franche-Comté, Dijon, France,

<sup>f</sup>INSERM, Dijon, France.

### **Footnotes**

\* Corresponding author: Tel.: +33 (0)380396273. Fax: +33 (0)380396250. E-mail address: stsavary@u-bourgogne.fr

**Abbreviations:** ABC, ATP-binding cassette; ACOX1, acyl-CoA oxidase 1; AMN, adrenomyeloneuropathy; cALD, cerebral adrenoleukodystrophy; CNS, central nervous system; CRISPR, clustered regularly interspaced short palindromic repeat; DAB, diaminobenzidine; FBS, fetal bovine serum; GC-MS, gas chromatography mass spectrometry; HDR, homologous directed repair; LPS, Lipopolysaccharide; L/VLCFA, long/very long-chain fatty acids; MUFA, monounsaturated fatty acids; NHEJ, non-homologous end-joining; PUFA, polyunsaturated fatty acids; SFA, saturated fatty acids; TEM, transmission electron microscopy; X-ALD, X-linked adrenoleukodystrophy.

**Keywords:** Adrenoleukodystrophy, Peroxisome, Microglia, ABC transporters, VLCFA

### **Abstract**

X-linked adrenoleukodystrophy (X-ALD), the most frequent peroxisomal disorder, is associated with mutation in the *ABCD1* gene which encodes a peroxisomal ATP-binding cassette transporter for very long-chain fatty acids (VLCFA). The biochemical hallmark of the disease is the accumulation of VLCFA. Peroxisomal defect in microglia being now considered a priming event in the pathology, we have therefore generated murine microglial cells mutated in the *Abcd1* gene and its closest homolog, the *Abcd2* gene. Using CRISPR/Cas9 gene editing strategy, we obtained 3 cell clones with a single or double deficiency. As expected, only the combined absence of ABCD1 and ABCD2 proteins resulted in the accumulation of VLCFA. Ultrastructural analysis by electron microscopy revealed in the double mutant cells the presence of lipid inclusions similar to those observed in brain macrophages of patients. These observations are likely related to the increased level of cholesterol and the accumulation of neutral lipids that we noticed in mutant cells. A preliminary characterization of the impact of peroxisomal defects on the expression of key microglial genes such as *Trem2* suggests profound changes in microglial functions related to inflammation and phagocytosis. The expression levels of presumed modifier genes have also been found modified in mutant cells, making these novel cell lines relevant for use as in vitro models to better understand the physiopathogenesis of X-ALD and to discover new therapeutic targets.

## 1 Introduction

X-linked adrenoleukodystrophy (X-ALD) is a neurodegenerative disorder caused by mutations in the *ABCD1* gene which encodes a peroxisomal ATP binding cassette (ABC) transporter [1, 2]. X-ALD is biochemically characterized by increased levels of saturated and monounsaturated straight chain very long-chain fatty acids (VLCFA) in brain, adrenal glands, and plasma. The disease presents two main clinical forms: the severe cerebral inflammatory form (cALD) mainly associated with childhood, and a less severe and slowly progressive adult form called adrenomyeloneuropathy (AMN). No correlation was found between mutations in the *ABCD1* gene and clinical forms of X-ALD suggesting the existence of modifier genes and/or environmental priming events related to inflammation. Thus, there is growing interest on the role of microglia, the resident immune cells of the central nervous system (CNS), in the pathogenesis of X-ALD. Constantly surveying their environment, these self-renewing and highly dynamic cells play a crucial role in the maintenance of the brain homeostasis [3]. Microglia responds to a broad range of environmental signals and this activation is often accompanied by morphologic and metabolic changes. Histological studies of X-ALD inflammatory lesions have highlighted reactive microgliosis with little involvement of lymphocyte infiltrates. Aberrant activation of microglia was suggested to be a consequence of the VLCFA accumulation with microglial cells undergoing apoptosis in the perilesional white matter [4]. Hematopoietic stem-cell transplantation (with or without gene correction) is currently the only effective therapy for cALD [5]. By replacing defective microglial cells and restoring their metabolic function in the CNS, non-mutant myeloid cells are thought to alleviate the neuroinflammatory response. More recently, microglia has been shown to contribute to the non-inflammatory lesion in the spinal cord of AMN patient, in link with a dysregulation of their phagocytosis function [6]. Microglia is therefore considered today as a central actor in both cALD and AMN.

Although evidence of the VLCFA accumulation acting as the inflammatory trigger is lacking, a higher VLCFA level has been measured in reactive cells in the lesion areas of cALD brain [7]. The exact link between VLCFA accumulation, demyelination, oxidative stress and inflammation as well as the sequence of events leading to the disease are still unclear. The *ABCD1* protein is involved in the import of CoA-esters of VLCFA into the peroxisome, the unique site of their  $\beta$ -oxidation. The *ABCD2* gene encodes a peroxisomal half-ABC transporter which is the closest homolog of *ABCD1* in mammals [8]. *ABCD1* and *ABCD2* proteins displaying overlapping substrate specificity and partial functional redundancy, overexpression of *ABCD2* has therefore been proposed as a therapeutic strategy for the treatment of X-ALD [9, 10]. Mice models with *Abcd1* or *Abcd2* mutations have been developed to further study these ABC transporters and provide a disease model [11-15]. The *Abcd1*-deficient mice appear clinically normal up to 6 months and start manifesting abnormal neurological symptoms after 15 months but do not display demyelinating features of cALD [11]. The *Abcd2*-deficient mice develop a late-onset cerebellar and sensory ataxia, with loss of cerebellar Purkinje cells and dorsal root ganglia cell degeneration [12]. As expected, the *Abcd1/Abcd2* double knockout mice demonstrated an accelerated and more severe neurological phenotype [9]. This increased severity in the double mutant was also confirmed from a metabolic point of view in mouse macrophages [16].

In addition to these animal models, the development of novel cell models of brain origin is definitely needed to better understand the link between metabolic defects and neurodegenerative processes in X-ALD. From the BV-2 immortalized cell line, which was established in 1990 [17] and which is recognized as a good alternative to primary microglial cells [18], we recently generated a microglial cell line with *Acox1* deficiency (*Acox1* encodes

the first and rate-limiting enzyme of peroxisomal  $\beta$ -oxidation) using CRISPR/Cas9 gene editing strategy [19]. The preliminary characterization of this mutant cell line has demonstrated its potential to facilitate the study of peroxisomal dysfunctions. BV-2 cells expressing both ABCD1 and ABCD2 proteins [20], the objective of the present study was to generate new BV-2-derived cell lines with single or double mutation in the *Abcd1* and *Abcd2* genes. Our strategy was based on the selection of non-homologous end-joining (NHEJ) repair events resulting in frameshift mutations following CRISPR/Cas9-mediated double strand DNA break [21]. Here, we present the establishment and the validation of 3 mutant cell clones (i.e. *Abcd1*-*Abcd2*- and *Abcd1/Abcd2*-deficient BV-2 cell clones) and their initial characterization focusing on cell growth, cell morphology and ultrastructure, and lipid content. Expression levels of key microglial genes and of genes suspected to be modifier genes in X-ALD were also analyzed.

## 2 Materials and methods

### 2.1 Plasmids

Custom synthesized plasmids used for genome editing were obtained from GeneCopoeia, Inc/tebu-bio (France). The all-in-one plasmids allow the co-expression of Cas9 nuclease, a mCherry fluorescent reporter, and one sgRNA targeting either the first exon of *Abcd1* (Catalog No: MCP226534-CG01-2-B-b; target sequence: 5'-GTCAGACACTGCCGTACTAG-3') or *Abcd2* (MCP230736-CG01-2-B-b; target sequence: 5'-GCTGCATTTAGTCCCGGCGC-3'). The specificity of CRISPR/Cas9 editing mainly depends on the sgRNA sequence and on the presence of protospacer adjacent motif located next to the target sequence. To avoid non-specific mutations, we paid attention to the design of the all-in-one CRISPR plasmid and relied on the expertise of our plasmid supplier. The sgRNA sequences were chosen to exhibit the highest quality score by inverse likelihood of off-target binding based on the CRISPR design tool developed by Zhang Lab, MIT 2017 (<http://crispr.mit.edu/>).

### 2.2 Cell culture, transfection, clonal selection, and proliferation assay

Murine microglial cells (BV-2) from female C57BL/6J mice purchased from Banca-Biologica e Cell Factory (catalog no. ATL03001) were cultured in DMEM supplemented with 10% heat-inactivated FBS and 1% penicillin/streptomycin (Dutscher). Cultures were maintained at 37 °C in a humidified atmosphere containing 5% CO<sub>2</sub>.

BV-2 cells ( $2 \times 10^6$ , ~70% confluence) were transfected with 2  $\mu$ g all-in-one plasmid using Amaxa Cell Line Nucleofector Kit T (Lonza) and program A-023. Twenty-four hours after transfection, adherent cells were gently detached using trypsin/EDTA, sorted by flow cytometry based on high expression of mCherry, and then seeded as single cells in a 96-well plate. Cells were allowed to grow for 10–14 days before genomic DNA extraction and genotyping. Between 5 and 20% of cells demonstrated survival and clonal amplification. Double-knockout cells were obtained after transfection of the selected *Abcd1*-deficient cell clone with the *Abcd2* all-in-one plasmid and selection with the same strategy.

For growth comparison, WT and mutant BV-2 cells were seeded in 24-well plates ( $2 \times 10^4$  cells/well) and cultivated for 24, 48, 72 or 96 h. The cells being semi-adherent, the medium was not replaced during growth to avoid cell loss. Viability was evaluated with trypan blue (0.025% final concentration). Living cells were counted using a hemocytometer. The average number of cells was obtained from triplicate of 3 independent experiments.

### 2.3 Molecular analysis (Genomic DNA purification, Indel detection, PCR)

Genomic DNA was extracted from selected clones or cellular pools with the NucleoSpin Tissue Kit (Macherey-Nagel). In order to assess CRISPR/Cas9 efficiency, detection of indels was first performed on a pool of transfected cells with T7 endonuclease assay (GeneCopoeia)

from PCR products obtained with the following primers for *Abcd1* locus (F: 5'-GGGCACCCCTAACTCGGACTC-3', R: 5'-GAAAGTGGCAGGAAGGGCGAT-3'), and *Abcd2* locus (F: 5'-TTCAAAGGGAAGAGGCCAGGAGT-3', R: 5'-TCCGAGGCTTCTTTCCACGATG-3'). After cell sorting, individual screening using PCR with GoTaq Flexi DNA polymerase (Promega) was performed with the following primer pairs: *Abcd1* (F: 5'-GGGCACCCCTAACTCGGACTC-3', R: 5'-GGAGTCAGACACTGCCGTA-3'), *Abcd2* (F: 5'-TTCAAAGGGAAGAGGCCAGGAGT-3', R: 5'-AGCTGCATTTAGTCCCGGCG-3'). The 3' end of each reverse primer was localized at the CRISPR/Cas9 targeted-mutation site. PCR products were visualized with ethidium bromide after electrophoresis on a gel containing 1.5% agarose and using a Bio-Rad Gel Doc XR+ Imager System. NHEJ mediated mutations were confirmed by Sanger sequencing (Eurofins Genomics Sanger sequencing platform, Germany) of PCR products amplified using GoTaq Flexi DNA polymerase (Promega) with the primers used for T7 endonuclease assay.

#### 2.4 Western blotting

Cell lysate preparation and western blotting were performed as previously described [19]. Briefly, detection of ABCD1 and ABCD2 was done using a rabbit polyclonal anti-ABCD1 antibody (1:5000; homemade serum 029 raised against the EQQLAGIPKMQGRLQELRQILGEAAAPVQPLVPGVPT, corresponding to amino acids 700–736 of mouse ABCD1 [22]), and a rabbit polyclonal anti-ABCD2 antibody (1:250; Abcam, ab102948), respectively. Actin was revealed using anti-actin antibody (dilution 1:10,000; Sigma-Aldrich). Following the incubation with the appropriate horseradish peroxidase (HRP)-conjugated secondary antibody (1:5000; Santa Cruz Biotechnology, Inc.), immunoreactivity was revealed by ECL (Santa Cruz Biotechnology). The membrane was first probed with the anti-ABCD1 or anti-ABCD2 antibody and then stripped by incubation for 30 min in stripping buffer (62.5 mM Tris-HCl pH 6.8, 2% SDS, 100 mM  $\beta$ -mercaptoethanol) at 50°C before being probed with the anti-actin antibody. Image processing and analysis were obtained using a Bio-Rad-Chemidoc XRS system.

#### 2.5 Optic and electron microscopy

The content of cellular neutral lipids was evaluated by staining cells with Oil Red O (Sigma-Aldrich) as previously described [19]. Transmission electron microscopy was used to visualize WT and mutant BV-2 cells cultured for 24 h. Cell sample preparation and diaminobenzidine-staining to visualize peroxisomes were performed as previously described [19]. Micrographs corresponding to 7–12 cells for each genotype, randomly taken from the grid, were analyzed by 6 different investigators in blind with a particular focus on the number of peroxisomes, mitochondria, and lipid vesicles and/or inclusions to give a score for each feature. Statistical analysis was performed from the analytical scores. Morphometry was performed from micrographs using ImageJ calculation of areas after manual delineation of organelles. The mean area ( $\pm$  SD) was expressed in  $\mu\text{m}^2$  and the maximum and minimum sizes were noted.

#### 2.6 Lipid analysis

The cholesterol and oxysterol levels as well as the fatty acid composition were measured by gas chromatography mass spectrometry (GC–MS) from cellular homogenates, prepared from pellets of  $10^7$  cells suspended in water (100  $\mu\text{l}$ ) and mixed with structural homologous internal standards (pentadecanoic and heptadecanoic acid, deuterium labeled sterols and oxysterols), as previously described [19, 23]. Peak integration was performed manually. Metabolites were recognized by retention time and fragmentation patterns, and quantified from

total-ion count against internal standards using standard curves for the measured fatty acids and sterols.

### 2.7 RTqPCR analysis

Total RNA was isolated from the BV-2 cells using the Qiagen RNeasy Mini kit and treated with DNase I. After quality and quantity control by spectrophotometry, RNA (1 µg) was reverse transcribed using the iScript cDNA Synthesis Kit (Bio-Rad). The synthesized cDNA was used as a template for Real-time PCR analysis using the SYBR Green real-time PCR technology and a StepOne Plus system (Applied Biosystems) as previously described [24].

*Trem2*, *Acsbg1*, *Mrc1*, *Cd1d1*, *Elovl7*, *Cybb*, and *Tyrobp* expression was quantified relatively to the expression of the house-keeping gene *36B4* using the following primers: *Trem2* (F: 5'-GACCTCTCCACCAGTTTCTCC-3', R: 5'-TACATGACACCCTCAAGGACTG-3'), *Acsbg1* (F: 5'-GGTGAATGCACACAGCAGATG-3', R: 5'-AATTAAGGAGCTGGTTTGGCGAGT-3'), *Mrc1* (F: 5'-GGAGGCTGATTACGAGCAGT-3', R: 5'-TGGTTCACCGTAAGCCCAATT-3'), *Cd1d1* (F: 5'-CCTTTGTGTACCAGTCCGGG-3', R: 5'-TTTTGCTGGGCTTCAGATTGTC-3'), *Elovl7* (F: 5'-CAAGAGCAATGAGGATGGTGC-3', R: 5'-GGTCCACGGCATGATCGTA-3'), *Cybb* (F: 5'-ACCCTCCTATGACTTGGAAATGG-3', R: 5'-CGAACCAACCTCTCACAAAGGT-3'), *Tyrobp* (F: 5'-CTCCTGACTGTGGGAGGATTAAG-3', R: 5'-CAATCCCAGCCAGTACACCA-3'), *36B4* (F: 5'-ATGGGTACAAGCGCGTCCTG-3', R: 5'-GCCTTGACCTTTTCAGTAAG-3').

### 2.8 Statistical analysis

Statistical analysis was performed using GraphPad Prism 5 software. One-way ANOVA followed by a Bonferroni post hoc test was used for every comparison between knockout genotypes versus WT. Two-way repeated measure ANOVA followed by a Bonferroni post hoc test was used for growth curves comparison. In all statistical tests, values of  $p < 0.05$  were considered significant.

## 3 Results

### 3.1 CRISPR-Cas9 knockout of *Abcd1* and *Abcd2* in BV-2 cells

Contrary to the HDR-based strategy previously used to generate *Acox1*-deficient BV-2 cells, which resulted in cell clones with the same mutation [19], BV-2 cells were only transfected with the all-in-one plasmids. Cells showing the higher expression level of mCherry 24 h after transfection were sorted by FACS and clonally cultivated before genomic analysis to check for mutations after non-homologous end-joining (NHEJ) repair events. Genotyping of individual cell clones was then carried out using specific primer pairs and demonstrated the loss of the WT allele (Fig. 1A). Sequencing of PCR products covering the respective *Abcd1* or *Abcd2* target locus confirmed mutations a few nucleotides after the start codon (Fig. 1B). In the *Abcd1*-deficient cell clone, two distinct frameshift mutations were identified (c.105delA and c.106insG). In the *Abcd2*-deficient cell clone, two distinct frameshift mutations were also identified (c.232delC and c.219\_231del). From the few cell clones demonstrating sufficient growth (approximately 10 per genotype), ~70% of cell clones containing no mutation, monoallelic, or biallelic mutations but without frameshift (deletion of 3 nucleotides), were not retained for further analysis.

At the end of each step, the selected mutant cell clones were expanded to generate a stock of cryogenic vials at the lowest passage. The selected *Abcd1*-deficient BV-2 cell clone was transfected with the *Abcd2* all-in-one plasmid to obtain the double knock-out cell clone and

the same screening strategy was applied. Genotyping confirmed the double disruption in only one of the 11 cell clones obtained. Surprisingly, Sanger sequencing demonstrated the presence of 3 distinct frameshift mutations in the *Abcd2* locus (c.232delC, c.231\_232del, c.212\_230del) (Fig. 1A). After excluding the hypothesis of sequencing/PCR artifacts, we hypothesized that these mutations are associated to multinuclearity and/or aneuploidy. We indeed observed multinucleated cells in culture, which is frequent in BV-2 and other microglial cells [25]. Besides, a recent study aiming to obtain mutant BV-2 cells for the *Trem2* gene also faced with triallelic mutations associated with cell multinuclearity and aneuploidy including trisomy of chromosome 17 [26]. Moreover, while *Abcd1* is located on the X chromosome [27], *Abcd2* is on the chromosome 15 [28], a chromosome whose trisomy is frequently found in murine cell lines, probably due to the location of c-myc [29].

Anyhow, the disruption of the *Abcd1* and/or *Abcd2* genes in the mutant cell clones was confirmed by western blot analysis demonstrating the absence of ABCD1 protein in the *Abcd1*-deficient cell clone, the absence of ABCD2 in the *Abcd2*-deficient cell clone, and the absence of both proteins in the double mutant cell clone (Fig. 2). Interestingly, we noticed a weak increase in ABCD1 ( $\times 1.77$  in the *Abcd2*<sup>-/-</sup> cells) and ABCD2 ( $\times 1.88$  in the *Abcd1*<sup>-/-</sup> cells) signals in the single mutants compared to the wild type suggesting possible compensation mechanisms.

### 3.2 Consequences of the absence of peroxisomal ABC transporters on fatty acid levels

In order to functionally validate the disruption of *Abcd1* and *Abcd2* genes, we conducted a lipid analysis to compare the fatty acid levels in WT and mutant cells with a particular focus on VLCFA. As said previously, *Abcd1* and *Abcd2* displaying a partial functional redundancy, accumulation of VLCFA was expected to occur only in the double mutant cell clone. This hypothesis has indeed been confirmed with a significant increase in the levels of C24:0, C26:0, C24:1 and C26:1 observed in the double mutant only (Table 1). The C24:0/C22:0 and C26:0/C22:0 ratio, which are used as diagnosis markers for X-ALD, remained unchanged in the single mutants and were respectively 1.6- and 5.1-fold higher than the control ones in the *Abcd1*<sup>-/-</sup>/*Abcd2*<sup>-/-</sup> cells (Fig. 3). As shown in Table 1, the total fatty acid level as well as the global quantity of the main species of fatty acids analyzed did not present significant differences between single mutant and control cells with the exception of PUFA in the *Abcd1* mutant cells. However, we observed increased levels of total FA, SFA, and PUFA in the *Abcd1*<sup>-/-</sup>/*Abcd2*<sup>-/-</sup> cells, statistical significance being obtained only for PUFA. Besides VLCFA, significant increase was observed for saturated LCFA (C18:0, C20:0, C22:0) and for some PUFA (C18:2 n-6, C20:3 n-6, C20:4 n-6 (arachidonic acid, AA) and C22:6 n-3 (docosahexaenoic acid, DHA)) while C20:5 n-3 was found decreased. The *Abcd1*<sup>-/-</sup> cells recapitulated partially these observations in particular in the PUFA series. In the *Abcd2*<sup>-/-</sup> cells, a significant increase was observed for C16:1 n-7 cis and C20:1 n-9 levels while C16:1 n-7 trans and C20:5 n-3 levels were found decreased.

### 3.3 Cell morphology and growth curve of BV-2 mutant cell lines

The *Acox1*-deficient BV-2 cell clone that we recently obtained and characterized was shown to grow slower than WT cells [19]. A similar result was obtained with the *Abcd1* and *Abcd2* mutated BV-2 cells cultivated over a period of 4 days in comparison with WT cells (Fig. 4). At 48 h, *Abcd1*<sup>-/-</sup> and *Abcd1*<sup>-/-</sup>/*Abcd2*<sup>-/-</sup> cells exhibited a significant growth retardation suggesting a slower division time. Growth retardation after 72 h of culture was significant for the three mutant cell clones, the *Abcd1*<sup>-/-</sup>/*Abcd2*<sup>-/-</sup> cells presenting the highest difference with the WT cells. Noteworthy, cell death of BV-2 mutant cells, quantified using trypan blue, did not differ from that of WT cells.

As in the case of *Acox1*-deficient BV-2 cells [19], we did not observe obvious

morphological differences between WT and mutant BV-2 cells (data not shown), the vast majority of cells adopting a round shape typical of a microglial activated status [30]. We further analyzed the mutant BV-2 cells by electron microscopy using diaminobenzidine (DAB) staining, which allows cytochemical detection of peroxisomes (Fig. 5). Score-based blind analysis of micrographs suggested a weak increase in the number of peroxisomes in *Abcd2*<sup>-/-</sup> and *Abcd1*<sup>-/-</sup>/*Abcd2*<sup>-/-</sup> cells and in the number of mitochondria in all mutant cells. A refined analysis did not demonstrate significant peroxisomal modification both in number and in size. However, it confirmed the increased number of mitochondria per micrographs ( $\times 1.95$  in *Abcd1*<sup>-/-</sup>,  $\times 1.46$  in *Abcd2*<sup>-/-</sup>, and  $\times 1.71$  in *Abcd1*<sup>-/-</sup>/*Abcd2*<sup>-/-</sup> cells). The size of mitochondria was moderately but significantly reduced in *Abcd1*<sup>-/-</sup> ( $0.435 \mu\text{m}^2 \pm 0.0196$ ,  $n = 133$ ) and in *Abcd1*<sup>-/-</sup>/*Abcd2*<sup>-/-</sup> ( $0.501 \mu\text{m}^2 \pm 0.0161$ ,  $n = 249$ ) cells as compared to WT cells ( $0.603 \pm 0.0342$ ,  $n = 113$ ). The mitochondrial size was however not significantly modified in the *Abcd2*<sup>-/-</sup> cells. Beyond these observations, the more striking differences concerned lipid droplets and lipid inclusions which appear in white in the micrographs (Fig. 5). The *Abcd1*<sup>-/-</sup> cells exhibit a significant increase in lipid droplets while *Abcd1*<sup>-/-</sup>/*Abcd2*<sup>-/-</sup> cells display a very unique striated pattern along with lamellar-lipid figures with a whorled or spiral form. These features prompted us to further examine cells with Oil Red O staining for the presence of neutral lipids. As shown in Fig. 6A, a more intense labeling was observed in *Abcd1*<sup>-/-</sup> cells and this increased staining was even more pronounced in *Abcd1*<sup>-/-</sup>/*Abcd2*<sup>-/-</sup> cells. Accumulation of neutral lipids, mainly cholesteryl-esters, represents a hallmark of peroxisomal disorders. To complete this analysis, we investigated whether total cholesterol level was modified in the mutant cells. Total cholesterol level was found significantly increased both in *Abcd1*<sup>-/-</sup> ( $\times 1.41$ ) and in *Abcd1*<sup>-/-</sup>/*Abcd2*<sup>-/-</sup> ( $\times 1.49$ ) cells but not significantly modified in *Abcd2*<sup>-/-</sup> cells (Fig. 6B). The lipid analysis was extended to oxysterols whose deleterious role in brain are predicted to participate in the pathogenesis of neurodegenerative disorders such as X-ALD [31, 32]. While  $7\alpha$ -hydroxycholesterol,  $7\beta$ -hydroxycholesterol,  $5\beta$ -cholestane- $3\alpha,7\alpha,12\alpha$ -triol and, to a lesser extent, 7-ketocholesterol, were almost not modified, we found increased levels of the two quantitatively major oxysterols (25-hydroxycholesterol and 27-hydroxycholesterol) in all mutant cells (Fig. 6C).

### 3.4 Expression of key microglial genes in the BV-2 mutant cell lines

Microglial cells ensure an important role in brain homeostasis by controlling inflammation and participating to phagocytosis of apoptotic cells and myelin debris. As a preliminary study of the functional consequences of *Abcd1* and *Abcd2* deficiency in the BV-2 cells, we investigated the mRNA levels of several genes associated with inflammation control and phagocytosis such as *Trem2* (Triggering receptor expressed by myeloid cells-2), *Tyrobp* (tyrosine kinase binding protein also called DNAX activating protein of 12 kDa, DAP12) and *Mrc1* (mannose receptor C-type 1, CD206). *Trem2* in association with DAP12 controls the phenotypic conversion of microglia and promotes phagocytosis [33]. *Mrc1* encodes a mannose receptor considered as a M2 polarization marker whose expression level was recently found decreased in cerebral adrenoleukodystrophy macrophages [34]. We also considered genes previously suspected to be modifier genes in X-linked adrenoleukodystrophy such as *Acsbg1*, which encodes a synthetase activating LCFA in the endoplasmic reticulum and playing an important role in brain [35], *Cd1d1* which encodes CD1d, a cell surface protein allowing lipid antigens to be presented to NKT lymphocytes [36] and genes encoding elongases responsible for the endogenous synthesis of VLCFA [37]. If the *Elovl1* gene is probably not a modifier gene since its expression level was found unchanged in primary peritoneal macrophages of *Abcd1/Abcd2* double-deficient mice [16], we focused on the *Elovl7* gene recently demonstrated to be controlled by the mTOR pathway [38], a pathway that governs autophagy mechanisms and is suspected to play a major role in X-ALD [39]. Alteration of redox homeostasis being

recognized as another main actor in the pathogenesis, we analyzed the expression of *Cybb* which encodes NOX2, a phagocytic NADPH oxidase highly expressed in microglia known to be implicated in many brain disorders and considered as one of the main sources of oxidants in this cell type [40]. As shown in Fig. 7, *Trem2* and *Tyrobp* expression levels were weakly increased in every mutant cells ( $\times 1.5$ – $\times 2.1$ ). *Mrc1* expression level was slightly decreased in the *Abcd1*<sup>-/-</sup>/*Abcd2*<sup>-/-</sup> cells ( $\times 0.6$ ), barely not modified in *Abcd1*<sup>-/-</sup> cells, and strikingly increased in the *Abcd2*<sup>-/-</sup> cells ( $\times 4.8$ ). *Cybb* expression was increased in the *Abcd1*<sup>-/-</sup> and the *Abcd1*<sup>-/-</sup>/*Abcd2*<sup>-/-</sup> cells ( $\times 1.6$  and  $\times 1.4$  respectively) which likely reflects oxidative stress in these cells. Concerning the putative modifier genes, in all the mutant cells, *Acsbg1* was slightly down-regulated ( $\times 0.4$ – $\times 0.8$ ) while both *Cd1d1* and *Elovl7* were strongly up-regulated.

## Discussion

In this study, our objective was to create a novel cell model useful in the context of X-ALD. Using CRISPR/Cas9 technology, we knocked out the *Abcd1* and *Abcd2* genes in BV-2 cells, a cell line commonly used as a substitute for primary microglia [18]. Contrarily to the *Acox1*-deficient cells that we generated using a strategy based on homologous directed recombination [19], here, we adopted a more direct strategy based on cell sorting and molecular screening of NHEJ events, strategy that has proven to be at least equally effective. We first confirmed mutations by DNA sequencing in the 3 cell clones as well as the correlated absence of ABCD1 and/or ABCD2 proteins by western blotting. Lipid analysis demonstrated the invalidation of peroxisomal ABC transporters in the double-mutant cells, the absence of both ABCD1 and ABCD2 proteins resulting in VLCFA accumulation (10-fold and 5-fold higher levels of C26:0 and C26:1 respectively in comparison with the respective levels in WT cells). Cross-compensation between ABCD1 and ABCD2 in single-deficient cells likely explains why VLCFA levels were not modified in single-mutant cells. These observations perfectly fit with what was observed in primary mouse peritoneal macrophages from *Abcd1* and *Abcd2* single- and double-deficient mice [16]. Of course, VLCFA accumulation could not be simply ascribed to the loss of peroxisomal  $\beta$ -oxidation. An increased endogenous synthesis of VLCFA, which depends on specific elongases encoded by *Elovl* genes, could also contribute to such accumulation. In favor of such explanation, we observed an increased expression of *Elovl7* in the mutant cells. Of note, like in human skin fibroblasts of X-ALD patients [41], the *Elovl1* expression remained almost unchanged (data not shown). In addition to VLCFA, surprisingly, we found several differences in saturated LCFA, MUFA as well as in PUFA levels. Peroxisomal defects in association with ABCD1 deficiency have proven to induce endoplasmic reticulum stress as well as mitochondrial defects [39, 42, 43]. Fatty acid elongation in the ER and oxidation in mitochondria may consequently be altered. In support to this hypothesis, we noticed that double-mutant cells exhibit a marked growth retardation as well as ultrastructural modifications concerning mitochondria (reduced size and increased number). The rare published data about lipid metabolism in BV-2 microglial cells have indicated that saturated LCFA levels are increased and MUFA levels are decreased upon LPS activation [44]. Further experiments will be necessary to determine whether the peroxisomal defect associated with the absence of ABCD1 and ABCD2 mimics such an activation state. Transcriptomic analysis of the mutant cell clones which is in progress may help to determine the effects on various genes associated with lipid metabolism (acyl-CoA synthetases, elongases, desaturases, ...). Concerning PUFA levels, both DHA and AA levels were found surprisingly increased in the *Abcd1*<sup>-/-</sup>/*Abcd2*<sup>-/-</sup> cells. DHA and AA are known precursors of signaling lipids playing mainly neuroprotective or proinflammatory roles, respectively [45, 46]. Profiling of VLCFA in phospholipids and lysophospholipids has recently revealed that specific PUFA are enriched in *Abcd1*-deficient mice [47]. Altogether, in-depth lipidomic analysis on membrane species,



cholesteryl esters and secreted lipids will be necessary to address the precise consequences of the mutations of the peroxisomal ABC transporters in the BV-2 microglial cells.

If we look specifically at the single mutant BV-2 cells, the *Abcd1*<sup>-/-</sup> cells did not demonstrate VLCFA accumulation and displayed a less-marked pattern than the double-mutant cells for LCFA, MUFA and PUFA. On the contrary, the *Abcd2*-deficient cells showed almost no change compared to WT cells, with the exception of increased levels of C16:1 n-7 (cis) and C20:1 n-9 and decreased levels of C16:1 n-7 (trans) and C20:5 n-3. Given the relatively high expression levels of both *Abcd1* and *Abcd2* genes in BV-2 cells [20], the known functional redundancy regarding saturated and monounsaturated fatty acids [9, 48], and the specificity of ABCD2 towards MUFA and PUFA [10, 22, 48-50], these results raise questions. Considering the divergences in the levels of several MUFA, PUFA and VLCFA levels observed in adrenals, spinal cord, sciatic nerve, or in primary neurons of *Abcd1*-, *Abcd2*- or *Abcd1/Abcd2* KO mice, the consequences of a deficiency in *Abcd1* and/or *Abcd2* seem strictly tissue and cell specific [49]. An overview of the enzymatic content of BV-2 microglial cells related to fatty acid metabolism is probably the key to understanding such observations. As mentioned above, the upcoming results of transcriptomic analysis will be helpful in that task. We can speculate that the observed increased levels of oxysterols in mutant cells might contribute to lipid changes resulting from LXR activation.

The *Abcd1*<sup>-/-</sup>/*Abcd2*<sup>-/-</sup> BV-2 cells were shown to reproduce the main biochemical feature of X-ALD (accumulation of VLCFA) and exhibit ultrastructural features resembling those observed in X-ALD patients. The observed striated pattern as well as the whorled lipid inclusions perfectly match with what was observed in adrenals, sural nerves, testis and macrophages of demyelinated areas of X-ALD patients [51, 52]. Such lipid inclusions were also described in the adrenals of *Abcd1/Abcd2* double KO mice [9] and are probably related to the accumulation of VLCFA-cholesteryl esters [53, 54]. The absence of such lipid figures in single mutant cells is likely associated to compensatory effects between ABCD1 and ABCD2 proteins. Oil Red O staining demonstrated accumulation of neutral lipids in the double mutant BV-2 cells and to a lesser extent in the *Abcd1*-deficient cells. These observations were correlated with increased levels of cholesterol. The exact link between cholesterol metabolism and peroxisomal functions is still under debate. It appears clear that cholesterol levels control the expression level of *Abcd2* [55-57] and interfere with saturated and monounsaturated VLCFA [58]. The consequences of peroxisomal defect on cholesterol metabolism have been more rarely described. Increased plasma level of cholesterol was observed in *Abcd1* KO mice [59] and cholesterol accumulation was observed in fibroblasts, adrenals, and cerebellum of *Abcd1* KO mice as well as in human fibroblasts from patients suffering from peroxisomal biogenesis disorders (Infantile Refsum disease and Zellweger syndrome) [50]. The blockage of cholesterol transport has been suggested to participate in peroxisomal pathologies [60]. Cholesterol, which may also serve as a substrate for oxidized derivatives responsible for deleterious effects in brain or as a modifier of membrane properties, could largely contribute to the neurodegenerative process in X-ALD in case of accumulation. The *Abcd1*<sup>-/-</sup>/*Abcd2*<sup>-/-</sup> BV-2 cells may therefore represent a very relevant in vitro model to answer these questions.

Preliminary investigations of the impact of the absence of peroxisomal ABC transporters in microglial BV-2 cells on gene expression have confirmed the utility of these new cellular models. First, we highlighted that the expression of *Trem2*, *Tyrobp* and *Mrc1* genes were modified suggesting, as in the case of *Acox1*-deficient cells [19], that phagocytosis ability is likely modified in the mutant cells. Further experiments will be necessary to evaluate the capacity of BV-2 mutant cells to engulf fluorescent beads, myelin debris or apoptotic cells, a microglial function that is considered to be a pathogenesis trigger event [6]. Besides the need to eliminate dying myelinating cells, phagocytosis has been shown to provide important signals for resolving inflammation. It will therefore be interesting to accompany further phagocytosis

analysis with a thorough examination of cytokine release and inflammatory pathways. In addition, the lipid characterization has shown modifications in several lipid species: fatty acids, cholesterol and oxysterols. Some oxysterols are known to display toxic effects in glial cells and are predicted to participate in neuroinflammatory process in X-ALD [31]. Since some of them result from auto-oxidation of cholesterol, their increased levels likely reflect oxidative stress. In accordance with this hypothesis of alteration of the redox homeostasis, *Cybb* was found up-regulated. *Cybb* actively participating in the cross talk between mitochondria and NADPH oxidases [61], serious disturbances related to mitochondrial functions are likely in mutant cells and deserve further analysis.

Concerning putative modifier genes, our results have shown that the *Acsbg1* gene is modestly down-regulated in every mutant cells. Although non statistically significant, these results perfectly match the decreased expression observed in the white matter of patients with AMN or cALD [35]. Concerning *Cd1d1* expression that was found strongly increased in mutant cells ( $\times 7.37$  in *Abcd1<sup>-/-</sup>/Abcd2<sup>-/-</sup>*), it suggests modifications in the ability of microglial cells to present lipid antigens to NKT cells. In patients, *CD1d* expression was found slightly decreased in B lymphocytes and unchanged in monocytes [62]. There was no difference in various cells of the *Abcd1* null mice [62] but *Cd1d1* expression was not investigated in *Abcd1/Abcd2* double-deficient mice. If *CD1d* polymorphism was positively associated with X-ALD, it failed to reach statistical significance like many linkage studies in rare disorders [36]. Our results suggest that further studies would be useful to test whether these results reflect species differences or confirm a role of *CD1d* in the pathology. Finally, *Elovl7* was found up-regulated in every mutant cells, particularly in the *Abcd1<sup>-/-</sup>* and *Abcd1<sup>-/-</sup>/Abcd2<sup>-/-</sup>* cells. A genome-wide association study concluded that *Elovl7* could be linked to multiple system atrophy, a progressive neurodegenerative disorder also known as Shy–Drager syndrome [63]. Further investigations in X-ALD patients should be carried out to confirm whether *Elovl7* is up-regulated and associated with the pathology.

## Conclusion

In summary, by using CRISPR/Cas9 editing, we have generated 3 mutant microglial cell lines mutated in *Abcd1* and/or *Abcd2* genes. Preliminary characterization of the double mutant cell clone has confirmed the main biochemical observations made in tissues from *Abcd1<sup>-/-</sup>* mice models and skin fibroblasts of X-ALD patients, i.e. the accumulation of VLCFA. Ultrastructure analysis in this cell clone demonstrated mitochondrial modifications as well as the presence of striated and whorled lipid inclusions similar to those observed in brain macrophages of X-ALD patients. Of note, the comparison of the double mutant with the single mutant cell clones that demonstrated mild or intermediate biochemical and cellular phenotypes, will represent a good opportunity to better understand the specific roles of peroxisomal ABC transporters ABCD1 and ABCD2 and the consequences of their defects in microglial cells. Expression levels of key microglial genes as well as putative modifier genes in the context of X-ALD were found modified. Transcriptomic RNAseq analysis is in progress to confirm these observations and reveal putative other dysregulated genes involved in RedOx homeostasis, inflammatory responses, and unexplored pathways in relation with microglial functions. These novel cell models will offer the advantage to test the impact of ABCD1 and/or ABCD2 deficiency in a key cell type for neurodegenerative process and to test original hypotheses on the involvement of peroxisome in phagocytosis, inflammatory and immune response. Microglial *Abcd1<sup>-/-</sup>/Abcd2<sup>-/-</sup>* cells will offer opportunities to further progress in the understanding of the physiopathogenesis of X-ALD. The cells will also offer the opportunity to set up screening assays to identify corrective molecules with a therapeutic potential for X-ALD.

## Acknowledgement

This work was supported by the Ministère de l'Education Nationale et de l'Enseignement Supérieur et de la Recherche (France) and by institutional grants from INSERM, CNRS and Aix-Marseille University to the CIML. Quentin Raas received a fellowship from ARSEP (Association for Research on Multiple Sclerosis). We thank the DImaCell platform for technical assistance in TEM (Microscopy Centre INRA/uB) and the cytometry platform of Dijon for cell sorting (INSERM/UB). We acknowledge the PICS imaging facility of the CIML (ImagImm), member of the national infrastructure France-BioImaging supported by the French National Research Agency (ANR-10-INBS-04). We thank Hai Tao He and Didier Marguet for hosting Quentin Raas for a few months at CIML.

## References

- [1] D. Trompier, S. Savary, X-linked Adrenoleukodystrophy, Morgan & Claypool Life Sciences, 2013.
- [2] J. Mosser, A.M. Douar, C.O. Sarde, P. Kioschis, R. Feil, H. Moser, A.M. Poustka, J.L. Mandel, P. Aubourg, Putative X-linked adrenoleukodystrophy gene shares unexpected homology with ABC transporters, *Nature* 361 (1993) 726-730.
- [3] D. Low, F. Ginhoux, Recent advances in the understanding of microglial development and homeostasis, *Cell. Immunol.* (2018).
- [4] F.S. Eichler, J.Q. Ren, M. Cossoy, A.M. Rietsch, S. Nagpal, A.B. Moser, M.P. Frosch, R.M. Ransohoff, Is microglial apoptosis an early pathogenic change in cerebral X-linked adrenoleukodystrophy?, *Ann. Neurol.* 63 (2008) 729-742.
- [5] N. Cartier, S. Hacein-Bey-Abina, C.C. Bartholomae, G. Veres, M. Schmidt, I. Kutschera, M. Vidaud, U. Abel, L. Dal-Cortivo, L. Caccavelli, N. Mahlaoui, V. Kiermer, D. Mittelstaedt, C. Bellesme, N. Lahlou, F. Lefrere, S. Blanche, M. Audit, E. Payen, P. Leboulch, B. l'Homme, P. Bougneres, C. Von Kalle, A. Fischer, M. Cavazzana-Calvo, P. Aubourg, Hematopoietic stem cell gene therapy with a lentiviral vector in X-linked adrenoleukodystrophy, *Science* 326 (2009) 818-823.
- [6] Y. Gong, N. Sasidharan, F. Laheji, M. Frosch, P. Musolino, R. Tanzi, D.Y. Kim, A. Biffi, J. El Khoury, F. Eichler, Microglial dysfunction as a key pathological change in adrenomyeloneuropathy, *Ann. Neurol.* 82 (2017) 813-827.
- [7] A.S. Paintlia, A.G. Gilg, M. Khan, A.K. Singh, E. Barbosa, I. Singh, Correlation of very long chain fatty acid accumulation and inflammatory disease progression in childhood X-ALD: implications for potential therapies., *Neurobiol. Dis.* 14 (2003) 425-439.
- [8] G. Lombard-Platet, S. Savary, C.O. Sarde, J.L. Mandel, G. Chimini, A close relative of the adrenoleukodystrophy (ALD) gene codes for a peroxisomal protein with a specific expression pattern, *Proc. Natl. Acad. Sci. U.S.A.* 93 (1996) 1265-1269.
- [9] A. Pujol, I. Ferrer, C. Camps, E. Metzger, C. Hindelang, N. Callizot, M. Ruiz, T. Pampols, M. Giros, J.L. Mandel, Functional overlap between ABCD1 (ALD) and ABCD2 (ALDR) transporters: a therapeutic target for X-adrenoleukodystrophy, *Hum. Mol. Genet.* 13 (2004) 2997-3006.
- [10] E. Genin, F. Geillon, C. Gondcaille, A. Athias, P. Gambert, D. Trompier, S. Savary, Substrate Specificity Overlap and Interaction between Adrenoleukodystrophy Protein (ALDP/ABCD1) and Adrenoleukodystrophy-related Protein (ALDRP/ABCD2), *J. Biol. Chem.* 286 (2011) 8075-8084.
- [11] A. Pujol, C. Hindelang, N. Callizot, U. Bartsch, M. Schachner, J.L. Mandel, Late onset neurological phenotype of the X-ALD gene inactivation in mice: a mouse model for adrenomyeloneuropathy., *Hum. Mol. Genet.* 11 (2002) 499-505.

- [12] I. Ferrer, J.P. Kapfhammer, C. Hindelang, S. Kemp, N. Troffer-Charlier, V. Broccoli, N. Callyzot, P. Mooyer, J. Selhorst, P. Vreken, R.J. Wanders, J.L. Mandel, A. Pujol, Inactivation of the peroxisomal ABCD2 transporter in the mouse leads to late-onset ataxia involving mitochondria, Golgi and endoplasmic reticulum damage, *Hum. Mol. Genet.* 14 (2005) 3565-3577.
- [13] S. Forss-Petter, H. Werner, J. Berger, H. Lassmann, B. Molzer, M.H. Schwab, H. Bernheimer, F. Zimmermann, K.A. Nave, Targeted inactivation of the X-linked adrenoleukodystrophy gene in mice, *J. Neurosci. Res.* 50 (1997) 829-843.
- [14] T. Kobayashi, N. Shinnoh, A. Kondo, T. Yamada, Adrenoleukodystrophy protein-deficient mice represent abnormality of very long chain fatty acid metabolism, *Biochem. Biophys. Res. Commun.* 232 (1997) 631-636.
- [15] J.F. Lu, A.M. Lawler, P.A. Watkins, J.M. Powers, A.B. Moser, H.W. Moser, K.D. Smith, A mouse model for X-linked adrenoleukodystrophy, *Proc. Natl. Acad. Sci. U. S. A.* 94 (1997) 9366-9371.
- [16] Z. Muneer, C. Wiesinger, T. Voigtlander, H.B. Werner, J. Berger, S. Forss-Petter, Abcd2 is a strong modifier of the metabolic impairments in peritoneal macrophages of abcd1-deficient mice, *PLoS ONE* 9 (2014) e108655.
- [17] E. Blasi, R. Barluzzi, V. Bocchini, R. Mazzolla, F. Bistoni, Immortalization of murine microglial cells by a v-raf/v-myc carrying retrovirus, *J. Neuroimmunol.* 27 (1990) 229-237.
- [18] A. Henn, S. Lund, M. Hedtjarn, A. Schratzenholz, P. Porzgen, M. Leist, The suitability of BV2 cells as alternative model system for primary microglia cultures or for animal experiments examining brain inflammation, *ALTEX* 26 (2009) 83-94.
- [19] Q. Raas, F.E. Saih, C. Gondcaille, D. Trompier, Y. Hamon, V. Leoni, C. Caccia, B. Nasser, M. Jadot, F. Menetrier, G. Lizard, M. Cherkaoui-Malki, P. Andreoletti, S. Savary, A microglial cell model for acyl-CoA oxidase 1 deficiency, *Biochim. Biophys. Acta* (2018).
- [20] M. Debbabi, T. Nury, I. Helali, E.M. Karym, F. Geillon, C. Gondcaille, D. Trompier, A. Najid, S. Terreau, M. Bezine, A. Zarrouk, A. Vejux, P. Andreoletti, M. Cherkaoui-Malki, S. Savary, G. Lizard, Flow Cytometric Analysis of the Expression Pattern of Peroxisomal Proteins, Abcd1, Abcd2, and Abcd3 in BV-2 Murine Microglial Cells, *Methods Mol. Biol.* 1595 (2017) 257-265.
- [21] M. Jinek, K. Chylinski, I. Fonfara, M. Hauer, J.A. Doudna, E. Charpentier, A programmable dual-RNA-guided DNA endonuclease in adaptive bacterial immunity, *Science* 337 (2012) 816-821.
- [22] F. Geillon, C. Gondcaille, S. Charbonnier, C.W. Van Roermund, T.E. Lopez, A.M.M. Dias, J.-P.P. de Barros, C. Arnould, R.J. Wanders, D. Trompier, S. Savary, Structure-Function Analysis of Peroxisomal ATP-binding Cassette Transporters Using Chimeric Dimers, *J. Biol. Chem.* 289 (2014) 24511-24520.
- [23] V. Leoni, T. Nury, A. Vejux, A. Zarrouk, C. Caccia, M. Debbabi, A. Fromont, R. Sghaier, T. Moreau, G. Lizard, Mitochondrial dysfunctions in 7-ketocholesterol-treated 158N oligodendrocytes without or with alpha-tocopherol: Impacts on the cellular profile of tricarboxylic cycle-associated organic acids, long chain saturated and unsaturated fatty acids, oxysterols, cholesterol and cholesterol precursors, *J. Steroid. Biochem. Mol. Biol.* 169 (2017) 96-110.
- [24] C. Gondcaille, E.C. Genin, T.E. Lopez, A.M.M. Dias, F. Geillon, P. Andreoletti, M. Cherkaoui-Malki, T. Nury, G. Lizard, I. Weinhofer, J. Berger, E.T. Kase, D. Trompier, S. Savary, LXR antagonists induce ABCD2 expression, *Biochim. Biophys. Acta* 1841 (2014) 259-266.
- [25] T.C. Hornik, U. Neniskyte, G.C. Brown, Inflammation induces multinucleation of Microglia via PKC inhibition of cytokinesis, generating highly phagocytic multinucleated giant cells, *J. Neurochem.* 128 (2014) 650-661.

- [26] Y.M. Lim, H. Rutter, R. Killick, A. Hodges, CRISPR/Cas9-mediated gene editing of TREM2 in monocytic and microglial cell lines, *Alzheimers Dement.* 13 (2017) P322.
- [27] M.A. Kennedy, S.A. Rowland, A.L. Miller, C.M. Morris, L.A. Neville, A. Dodd, W.J. Fifield, D.R. Love, Structure and location of the murine adrenoleukodystrophy gene, *Genomics* 32 (1996) 395-400.
- [28] S. Savary, N. Troffer-Charlier, G. Gyapay, M. Mattei, G. Chimini, Chromosomal localization of the adrenoleukodystrophy-related gene in man and mice, *Europ. J. Hum. Genet.* 5 (1997) 99-101.
- [29] M. Banerjee, F. Wiener, J. Spira, M. Babonits, M.G. Nilsson, J. Sumegi, G. Klein, Mapping of the c-myc, pvt-1 and immunoglobulin kappa genes in relation to the mouse plasmacytoma-associated variant (6;15) translocation breakpoint, *EMBO J.* 4 (1985) 3183-3188.
- [30] M.A. Laurenzi, C. Arcuri, R. Rossi, P. Marconi, V. Bocchini, Effects of microenvironment on morphology and function of the microglial cell line BV-2, *Neurochem. Res.* 26 (2001) 1209-1216.
- [31] J. Jang, S. Park, H. Jin Hur, H.J. Cho, I. Hwang, Y. Pyo Kang, I. Im, H. Lee, E. Lee, W. Yang, H.C. Kang, S. Won Kwon, J.W. Yu, D.W. Kim, 25-hydroxycholesterol contributes to cerebral inflammation of X-linked adrenoleukodystrophy through activation of the NLRP3 inflammasome, *Nat. Commun.* 7 (2016) 13129.
- [32] V. Mutemberezi, O. Guillemot-Legris, G.G. Muccioli, Oxysterols: From cholesterol metabolites to key mediators, *Prog. Lipid Res.* 64 (2016) 152-169.
- [33] T.R. Jay, V.E. von Saucken, G.E. Landreth, TREM2 in neurodegenerative diseases, *Mol. Neurodegener.* 12 (2017) 56.
- [34] I. Weinhofer, B. Zierfuss, S. Hametner, M. Wagner, N. Popitsch, C. Machacek, B. Bartolini, G. Zlabinger, A. Ohradanova-Repic, H. Stockinger, W. Kohler, R. Hoftberger, G. Regelsberger, S. Forss-Petter, H. Lassmann, J. Berger, Impaired plasticity of macrophages in X-linked adrenoleukodystrophy, *Brain* (2018).
- [35] M. Asheuer, I. Bieche, I. Laurendeau, A. Moser, B. Hainque, M. Vidaud, P. Aubourg, Decreased expression of ABCD4 and BG1 genes early in the pathogenesis of X-linked adrenoleukodystrophy, *Hum. Mol. Genet.* 14 (2005) 1293-1303.
- [36] M. Barbier, A. Sabbagh, E. Kasper, M. Asheuer, O. Ahouansou, I. Pribill, S. Forss-Petter, M. Vidaud, J. Berger, P. Aubourg, CD1 gene polymorphisms and phenotypic variability in X-linked adrenoleukodystrophy, *PLoS ONE* 7 (2012) e29872.
- [37] A. Kihara, Very long-chain fatty acids: elongation, physiology and related disorders, *J. Biochem.* 152 (2012) 387-395.
- [38] J.G. Purdy, T. Shenk, J.D. Rabinowitz, Fatty acid elongase 7 catalyzes lipidome remodeling essential for human cytomegalovirus replication, *Cell Rep.* 10 (2015) 1375-1385.
- [39] N. Launay, C. Aguado, S. Fourcade, M. Ruiz, L. Grau, J. Riera, C. Guilera, M. Giros, I. Ferrer, E. Knecht, A. Pujol, Autophagy induction halts axonal degeneration in a mouse model of X-adrenoleukodystrophy, *Acta Neuropathol. (Berl)* 129 (2015) 399-415.
- [40] F. Vilhardt, J. Haslund-Vinding, V. Jaquet, G. McBean, Microglia antioxidant systems and redox signalling, *Br. J. Pharmacol.* 174 (2017) 1719-1732.
- [41] R. Ofman, I.M. Dijkstra, C.W. van Roermund, N. Burger, M. Turkenburg, A. van Cruchten, C.E. van Engen, R.J. Wanders, S. Kemp, The role of ELOVL1 in very long-chain fatty acid homeostasis and X-linked adrenoleukodystrophy, *EMBO Mol. Med.* 2 (2010) 90-97.
- [42] J. Lopez-Erauskin, J. Galino, P. Bianchi, S. Fourcade, A.L. Andreu, I. Ferrer, C. Munoz-Pinedo, A. Pujol, Oxidative stress modulates mitochondrial failure and cyclophilin D function in X-linked adrenoleukodystrophy, *Brain* 135 (2012) 3584-3598.

- [43] S. Fourcade, J. Lopez-Erauskin, M. Ruiz, I. Ferrer, A. Pujol, Mitochondrial dysfunction and oxidative damage cooperatively fuel axonal degeneration in X-linked adrenoleukodystrophy, *Biochimie* 98 (2014) 143-149.
- [44] E.B. Button, A.S. Mitchell, M.M. Domingos, J.H. Chung, R.M. Bradley, A. Hashemi, P.M. Marvyn, A.C. Patterson, K.D. Stark, J. Quadrilatero, R.E. Duncan, Microglial cell activation increases saturated and decreases monounsaturated fatty acid content, but both lipid species are proinflammatory, *Lipids* 49 (2014) 305-316.
- [45] S. Savary, D. Trompier, P. Andreoletti, F. Le Borgne, J. Demarquoy, G. Lizard, Fatty Acids - Induced Lipotoxicity and Inflammation, *Curr. Drug Metab.* 13 (2012) 1358-1370.
- [46] N.G. Bazan, Docosanoids and eovanoids from omega-3 fatty acids are pro-homeostatic modulators of inflammatory responses, cell damage and neuroprotection, *Mol. Aspects Med.* (2018).
- [47] K. Hama, Y. Fujiwara, M. Morita, F. Yamazaki, Y. Nakashima, S. Takei, S. Takashima, M. Setou, N. Shimosawa, T. Imanaka, K. Yokoyama, Profiling and Imaging of Phospholipids in Brains of Abcd1-Deficient Mice, *Lipids* 53 (2018) 85-102.
- [48] C.W. van Roermund, W.F. Visser, L. Ijlst, H.R. Waterham, R.J. Wanders, Differential substrate specificities of human ABCD1 and ABCD2 in peroxisomal fatty acid beta-oxidation, *Biochim. Biophys. Acta* 1811 (2011) 148-152.
- [49] S. Fourcade, M. Ruiz, C. Camps, A. Schluter, S.M. Houten, P.A. Mooyer, T. Pampols, G. Dacremont, R.J. Wanders, M. Giros, A. Pujol, A key role for the peroxisomal ABCD2 transporter in fatty acid homeostasis, *Am. J. Physiol. Endocrinol. Metab.* 296 (2009) E211-221.
- [50] J. Liu, N.S. Sabeva, S. Bhatnagar, X.A. Li, A. Pujol, G.A. Graf, ABCD2 is abundant in adipose tissue and opposes the accumulation of dietary erucic acid (C22:1) in fat, *J. Lipid Res.* 51 (2010) 162-168.
- [51] H.H. Schaumburg, J.M. Powers, K. Suzuki, C.S. Raine, Adreno-leukodystrophy (sex-linked Schilder disease). Ultrastructural demonstration of specific cytoplasmic inclusions in the central nervous system, *Arch. Neurol.* 31 (1974) 210-213.
- [52] J.M. Powers, H.H. Schaumburg, Adreno-leukodystrophy (sex-linked Schilder's disease). A pathogenetic hypothesis based on ultrastructural lesions in adrenal cortex, peripheral nerve and testis, *Am. J. Pathol.* 76 (1974) 481-491.
- [53] M. Igarashi, H.H. Schaumburg, J. Powers, Y. Kishimoto, E. Kolodny, K. Suzuki, Fatty acid abnormality in adrenoleukodystrophy, *J. Neurochem.* 26 (1976) 851-860.
- [54] G. Kellner-Weibel, B. McHendry-Rinde, M.P. Haynes, S. Adelman, Evidence that newly synthesized esterified cholesterol is deposited in existing cytoplasmic lipid inclusions, *J. Lipid Res.* 42 (2001) 768-777.
- [55] D. Trompier, C. Gondcaille, G. Lizard, S. Savary, Regulation of the adrenoleukodystrophy-related gene (ABCD2): Focus on oxysterols and LXR antagonists, *Biochem. Biophys. Res. Commun.* 446 (2014) 651-655.
- [56] I. Weinhofer, S. Forss-Petter, M. Zigman, J. Berger, Cholesterol regulates ABCD2 expression: implications for the therapy of X-linked adrenoleukodystrophy, *Hum. Mol. Genet.* 11 (2002) 2701-2708.
- [57] I. Weinhofer, M. Kunze, H. Rampler, A.L. Bookout, S. Forss-Petter, J. Berger, Liver X receptor alpha interferes with SREBP1c-mediated Abcd2 expression. Novel cross-talk in gene regulation, *J. Biol. Chem.* 280 (2005) 41243-41251.
- [58] M. Engelen, R. Ofman, P.A. Mooijer, B.T. Poll-The, R.J. Wanders, S. Kemp, Cholesterol-deprivation increases mono-unsaturated very long-chain fatty acids in skin fibroblasts from patients with X-linked adrenoleukodystrophy, *Biochim. Biophys. Acta* 1781 (2008) 105-111.

- [59] I. Weinhofer, S. Forss-Petter, M. Kunze, M. Zigman, J. Berger, X-linked adrenoleukodystrophy mice demonstrate abnormalities in cholesterol metabolism, *FEBS Lett.* 579 (2005) 5512-5516.
- [60] B.B. Chu, Y.C. Liao, W. Qi, C. Xie, X. Du, J. Wang, H. Yang, H.H. Miao, B.L. Li, B.L. Song, Cholesterol transport through lysosome-peroxisome membrane contacts, *Cell* 161 (2015) 291-306.
- [61] S. Dikalov, Cross talk between mitochondria and NADPH oxidases, *Free Radic. Biol. Med.* 51 (2011) 1289-1301.
- [62] A.S. Gautron, B. Giquel, L. Beaudoin, E. Autrusseau, A. Speak, F. Platt, S. Kemp, A. Pujol, P. Aubourg, A. Lehuen, Invariant NKT cells in adrenoleukodystrophy patients and mice, *J. Neuroimmunol.* 229 (2010) 204-211.
- [63] A. Sailer, S.W. Scholz, M.A. Nalls, C. Schulte, M. Federoff, T.R. Price, A. Lees, O.A. Ross, D.W. Dickson, K. Mok, N.E. Mencacci, L. Schottlaender, V. Chelban, H. Ling, S.S. O'Sullivan, N.W. Wood, B.J. Traynor, L. Ferrucci, H.J. Federoff, T.R. Mhyre, H.R. Morris, G. Deuschl, N. Quinn, H. Widner, A. Albanese, J. Infante, K.P. Bhatia, W. Poewe, W. Oertel, G.U. Hoglinger, U. Wullner, S. Goldwurm, M.T. Pellecchia, J. Ferreira, E. Tolosa, B.R. Bloem, O. Rascol, W.G. Meissner, J.A. Hardy, T. Revesz, J.L. Holton, T. Gasser, G.K. Wenning, A.B. Singleton, H. Houlden, G. European Multiple System Atrophy Study, U.K.M.S.A.S.G. the, A genome-wide association study in multiple system atrophy, *Neurol.* 87 (2016) 1591-1598.

## Figure Legends

**Fig. 1.** CRISPR/Cas9-mediated knockout of *Abcd1* and *Abcd2* genes in BV-2 cells. (A) Agarose gel electrophoresis of PCR products illustrating indel screening of individual BV-2 cell clones. The 3' end of the reverse primer corresponding to the CRISPR targeted site, absence of PCR amplification indicates a disrupted site (1: negative control; 2: wild type BV-2 cells; 3: *Abcd1*<sup>-/-</sup> cell clone; 4: *Abcd2*<sup>-/-</sup> cell clone; 5: *Abcd1*<sup>-/-</sup>/*Abcd2*<sup>-/-</sup> cell clone). (B) Schematic representation of the *Abcd1* and *Abcd2* locus showing exon organization and sgRNA target sites (in exon 1) with their respective sequences in bold. The protospacer adjacent motif (NGG on the complementary strand) which allows specific binding and cleavage by the Cas9 nuclease is boxed. Nucleotide sequences are numbered from the translation start codon and translated sequences are indicated. The position of the reverse primer used for indel screening is indicated by the arrow. Below are presented the sequences of the *Abcd1* and *Abcd2* exon 1 in mutant cell clones demonstrating frame shift insertions or deletions (in bold). The *Abcd1*<sup>-/-</sup>/*Abcd2*<sup>-/-</sup> cell clone and the *Abcd1*<sup>-/-</sup> clone from which it was obtained, exhibit the same mutations in the *Abcd1* locus.

**Fig. 2.** Western blot analysis of ABCD1 and ABCD2 expression in mutant BV-2 cells. Whole cell lysates were separated on 7.5% SDS-PAGE, blotted on PVDF membrane and analyzed by immunoblotting with anti-ABCD1 (homemade serum 029), anti-ABCD2 (Abcam, ab102948) and anti-Actin antibodies.

**Fig. 3.** VLCFA accumulate in *Abcd1*<sup>-/-</sup>/*Abcd2*<sup>-/-</sup> BV-2 cells but not in ABCD1 or ABCD2 single mutants. FA content of BV-2 cells was measured by GC/MS. C26:0 and C24:0 values are normalized to C22:0 values (mean with SD of three independent experiments, ANOVA with Bonferroni post-hoc test; \*\*\* P value < 0.001).

**Fig. 4.** Proliferation curves of mutant BV-2 cells. At t0, 2×10<sup>4</sup> cells were seeded. Data represent mean values of 3 independent experiments (cells, from the same passage number, thawed at different dates and cultivated during 48 h) with 3 technical replicates ± SD. Statistically significant differences with WT cells determined by ANOVA with Bonferroni post-hoc test are indicated: \*\*\* P value < 0.001.

**Fig. 5.** Ultrastructure analysis of mutant BV-2 cells. Transmission electron micrographs (whole cell and respective higher magnification) of WT (A and B), *Abcd1*<sup>-/-</sup> (C and D), *Abcd2*<sup>-/-</sup> (E and F), and *Abcd1*<sup>-/-</sup>/*Abcd2*<sup>-/-</sup> (G and H) BV-2 cells (bar = 2 μm). Peroxisomes and lipid droplets are indicated (arrowheads and short arrows respectively). Striated and whorled lipid inclusions, characteristic features of X-ALD, are present in the double mutant cells.

**Fig. 6.** Lipid accumulation in mutant BV-2 cells. (A) Light microscopic images of Oil Red O staining in WT, *Abcd1*<sup>-/-</sup>, *Abcd2*<sup>-/-</sup>, and *Abcd1*<sup>-/-</sup>/*Abcd2*<sup>-/-</sup> BV-2 cells (bar = 20 μm). Total cholesterol (μg/mg of protein) (B) and oxysterol levels (ng /mg of protein) (C) in BV-2 cells measured by GC/MS and normalized to protein content. Data represent the mean values ± SD of 3 independent experiments. Statistically significant differences determined by ANOVA with Bonferroni post-hoc test are indicated: \*\*\* P value < 0.001, \*\* P value < 0.01, \* P value < 0.05.

**Fig. 7.** Relative mRNA levels of key microglial genes in mutant BV-2 cells. Expression levels of genes involved in microglial functions and phagocytosis (genes encoding the immune receptor Trem2 and its membrane partner, DAP12 (*Tyrobp*), as well as the mannose receptor MRC1/CD206), putative modifier genes in X-ALD (*Acsbg1*, *Cd1d1* and *Elovl7*), and *Cybb*,



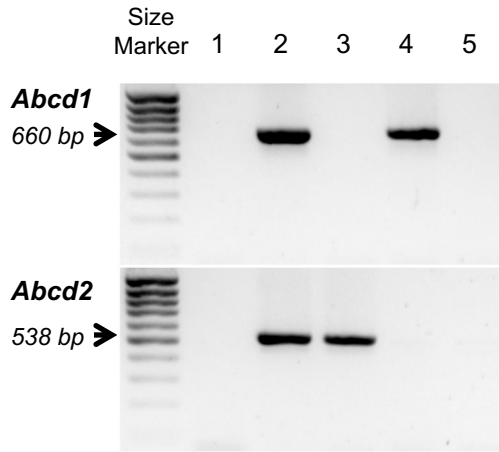
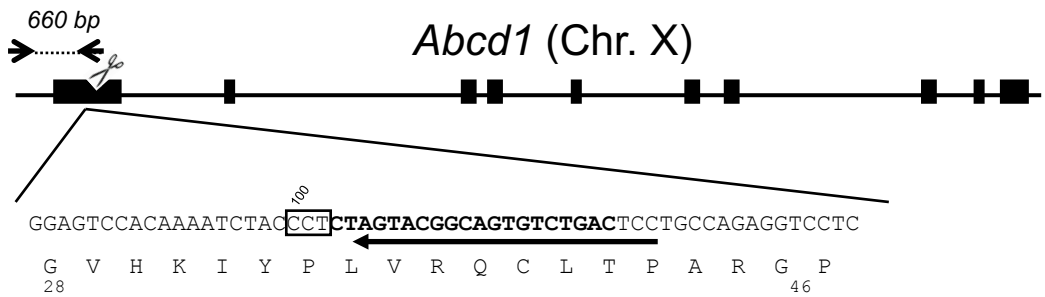
which encodes one of the most expressed NADPH oxidase in microglia (NOX2)), were measured using RT-qPCR and normalized to *36B4*. Data represent the mean values  $\pm$  SD of 3 independent experiments and are expressed as relative expression levels in comparison with the corresponding expression level in WT cells taken arbitrary equal to 1. Statistically significant differences determined by ANOVA with Bonferroni post-hoc test are indicated: \*\*\* P value < 0.001, \*\* P value < 0.01, \* P value < 0.05.

**Table 1.** Fatty acid levels in WT and mutant BV-2 cells cultivated during 48h.

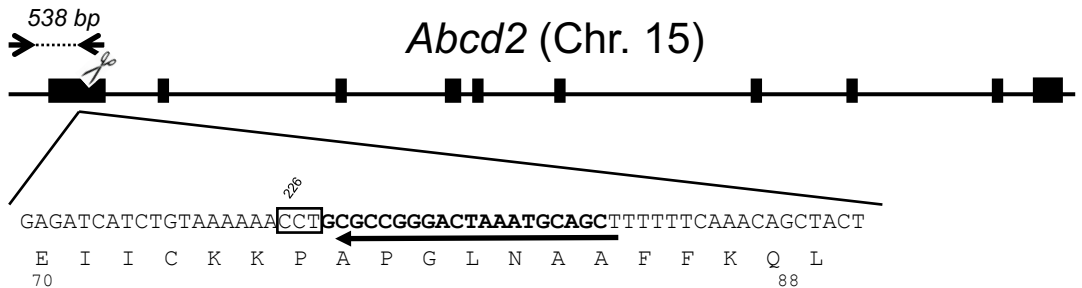
	WT		<i>Abcd1</i> <sup>-/-</sup>		<i>Abcd2</i> <sup>-/-</sup>		<i>Abcd1</i> <sup>-/-</sup> / <i>Abcd2</i> <sup>-/-</sup>		
	Mean	SD	Mean	SD	Mean	SD	Mean	SD	
<b>C16:0</b>	17,716	2255	18,884	1789	18,890	5239	23,959	817	
<b>C18:0</b>	9925	1425	12,311	482	9704	1817	14,346	1055	*
<b>C20:0</b>	91.1	17.6	148	18.2	* 76.8	26.4	289	15.2	***
<b>C22:0</b>	28.9	5.68	35.5	3.27	26.1	6.61	55.4	7.20	**
<b>C24:0</b>	62.0	6.26	71.2	4.52	56.5	15.7	189	19.0	***
<b>C26:0</b>	11.6	3.68	15.8	1.69	9.24	2.85	114	9.58	***
<b>SFA</b>	27,834	3684	31,465	2247	28,763	7091	38,952	1850	
<b>C16:1 n-7 trans</b>	1637	412	924	129	* 608	201	** 1064	71.0	
<b>C16:1 n-7 cis</b>	5468	549	8718	658	9078	2153	* 8825	876	
<b>C18:1 n-9</b>	24,135	2902	21,867	1789	18,069	3128	22,416	1213	
<b>C18:1 n-7</b>	11,012	860	15,817	1503	16,184	3953	11,704	455	
<b>C20:1 n-9</b>	329	22.4	472	55.6	623	105	** 406	31.4	
<b>C22:1 n-9</b>	41.5	4.97	34.6	3.10	48.3	11.7	48.0	3.46	
<b>C24:1 n-9</b>	58.0	7.50	64.8	4.34	61.6	17.8	134	7.52	***
<b>C26:1 n-9</b>	15.4	2.40	19.9	1.20	13.7	3.73	76.6	3.60	***
<b>MUFA</b>	42,695	4162	47,917	3812	44,685	9500	44,673	2560	
<b>C18:2 n-6</b>	778	147	2079	229	*** 1051	285	2567	92.0	***
<b>C20:3 n-6</b>	742	92.8	765	78.5	625	93.3	1261	42.2	***
<b>C20:4 n-6</b>	2258	275	3781	441	** 2347	273	5252	409	***
<b>C20:5 n-3</b>	1478	160	561	98.7	*** 478	80.6	*** 948	48.4	**
<b>C22:6 n-3</b>	1579	129	2425	224	** 1441	197	2744	147	***
<b>PUFA</b>	6836	778	9611	1066	* 5942	924	12,772	671	***
<b>Total FA</b>	77,365	8552	88,993	6921	79,390	17,422	96,397	4987	

Data represent mean levels of fatty acids (saturated (SFA), monounsaturated (MUFA), and polyunsaturated (PUFA)) measured by GC/MS and expressed in ng/mg of protein of 3 independent experiments with their respective standard deviation (SD).

Significant differences at  $p < 0.001$ \*\*\*,  $p < 0.01$ \*\* ,  $p < 0.05$ \* determined by ANOVA followed by Bonferroni post-hoc test are indicated.

**A****B***Abcd1*<sup>-/-</sup> and *Abcd1*<sup>-/-</sup>/*Abcd2*<sup>-/-</sup>

GGAGTCCACAAAATCTACCTCT-GTACGGCAGTGTCTGACTCCTGCCAGAGGTCCTC c.105delA  
 GGAGTCCACAAAATCTACCTCTAGGTACGGCAGTGTCTGACTCCTGCCAGAGGTCCTC c.106insG

*Abcd2*<sup>-/-</sup>

GAGATCATCTGTAAAAAACCTGCG-CGGGACTAAATGCAGCTTTTTTCAAACAGCTACT c.232delC  
 GAGATCATCTG-----CCGGGACTAAATGCAGCTTTTTTCAAACAGCTACT c.219\_231del

*Abcd1*<sup>-/-</sup>/*Abcd2*<sup>-/-</sup>

GAGATCATCTGTAAAAAACCTGCG-CGGGACTAAATGCAGCTTTTTTCAAACAGCTACT c.232delC  
 GAGATCATCTGTAAAAAACCTGC--CGGGACTAAATGCAGCTTTTTTCAAACAGCTACT c.231\_232del  
 GAGA-----GCCGGGACTAAATGCAGCTTTTTTCAAACAGCTACT c.212\_230del

**Fig.1**

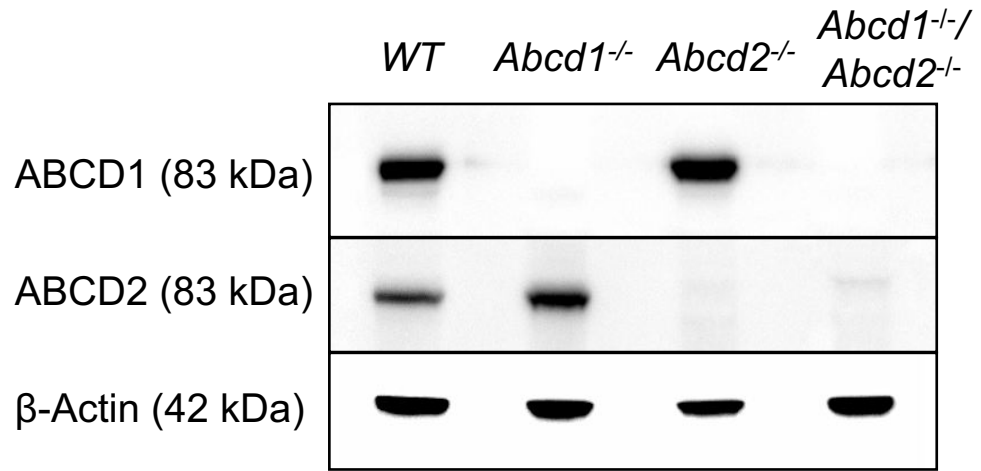


**Fig.2**

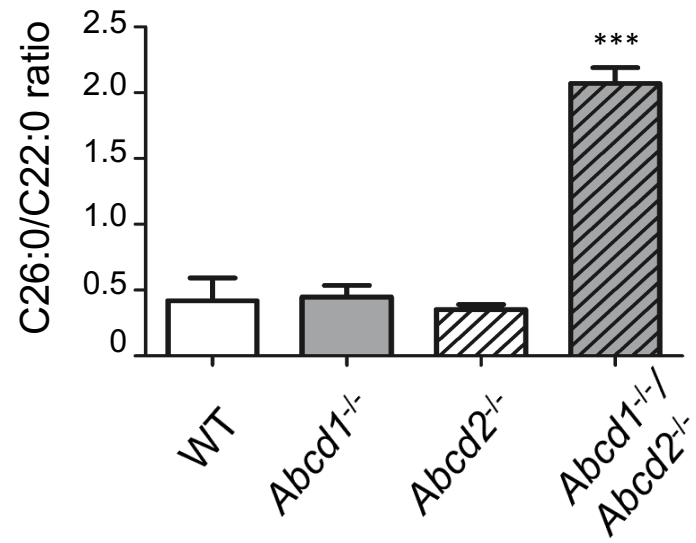
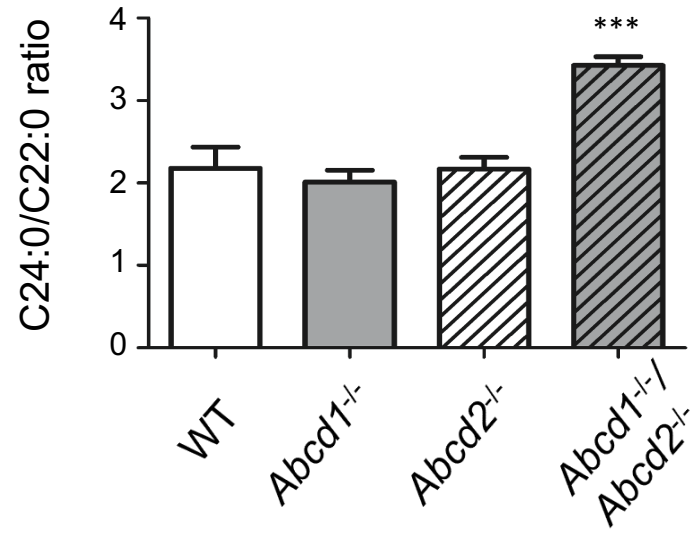


**Fig. 3**

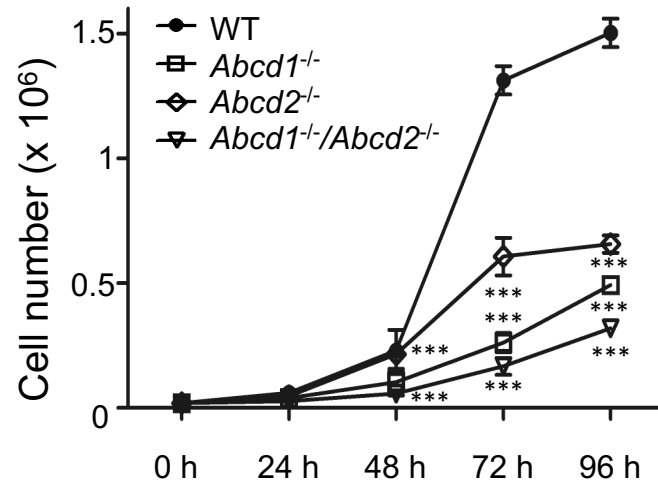


**Fig. 4**

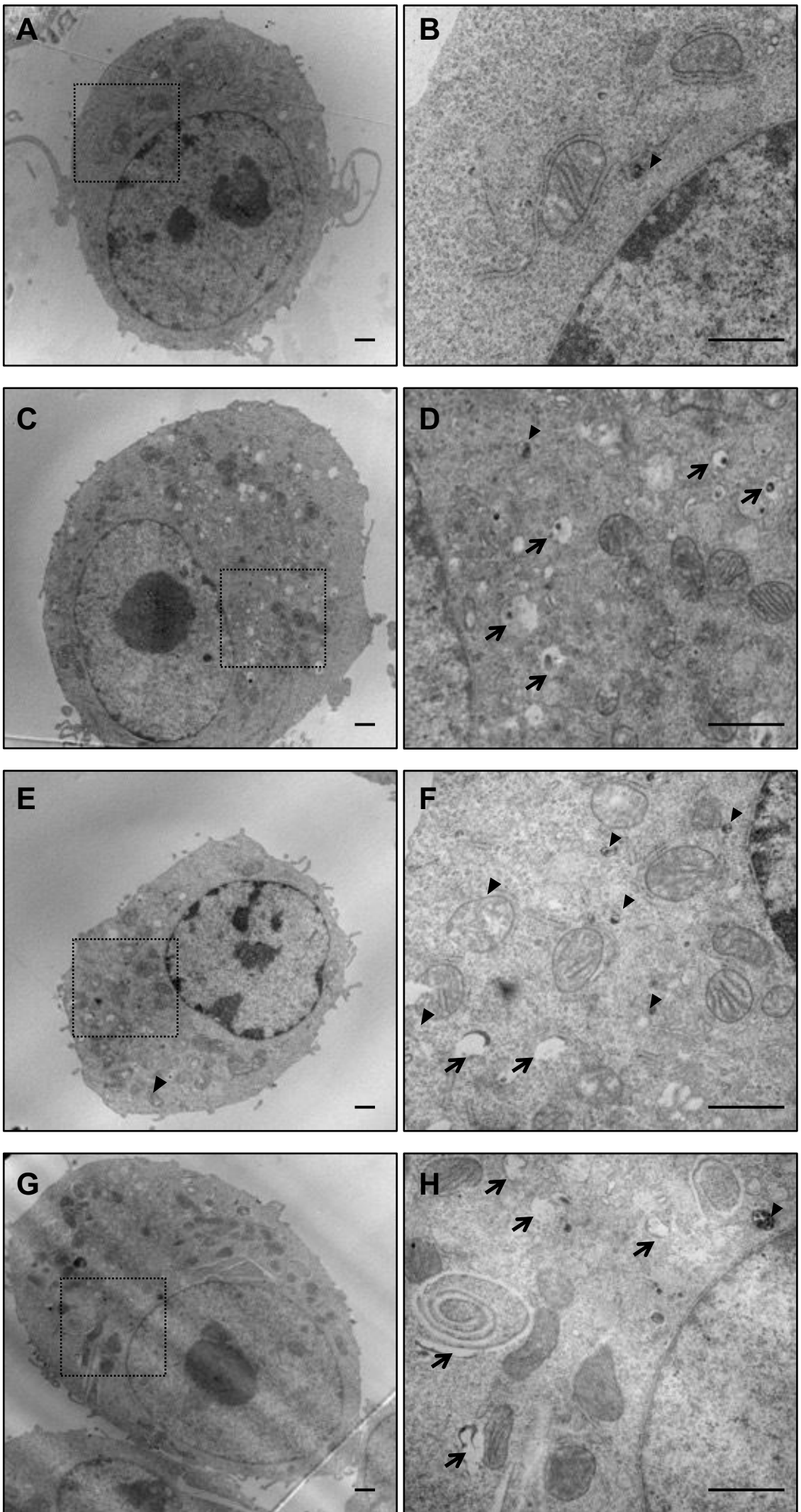


**Fig. 5**

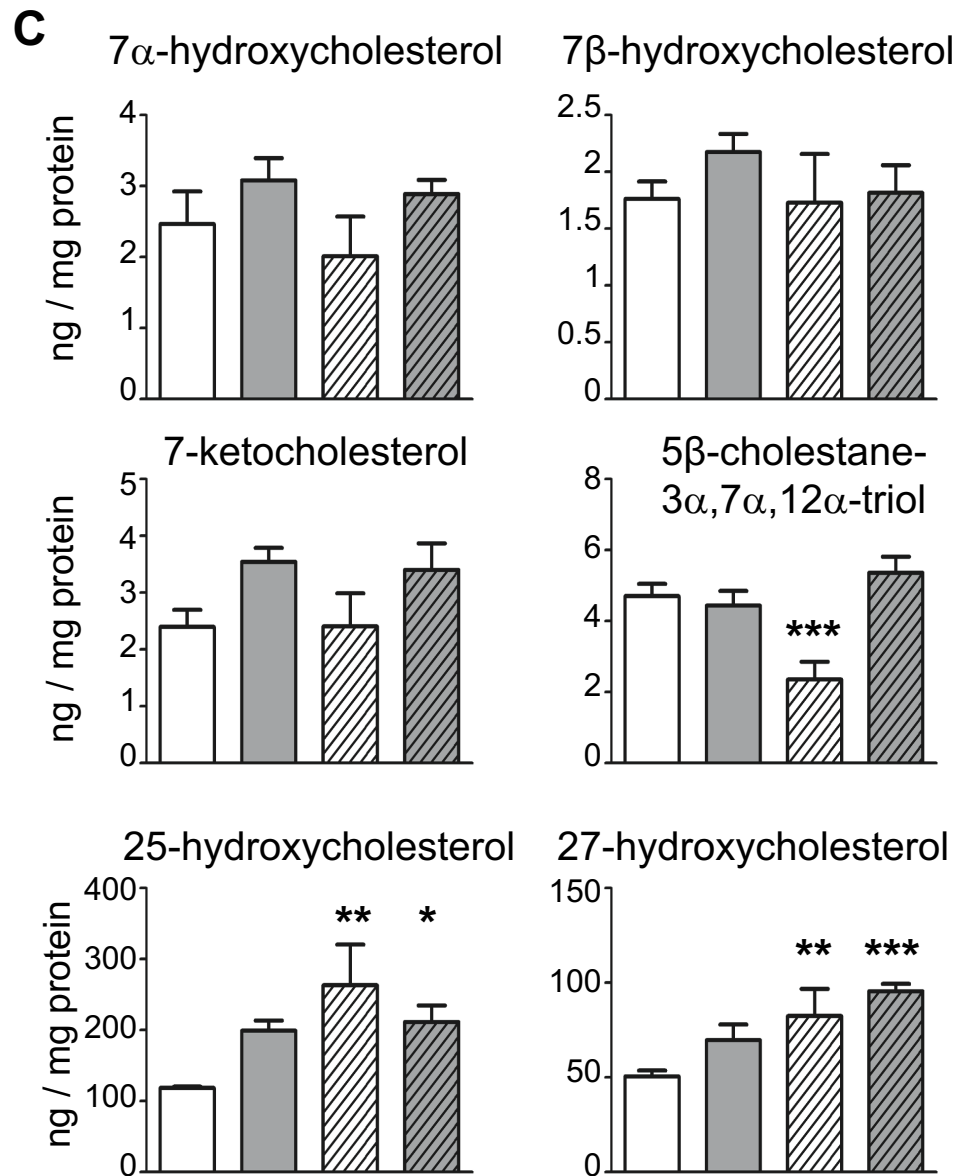
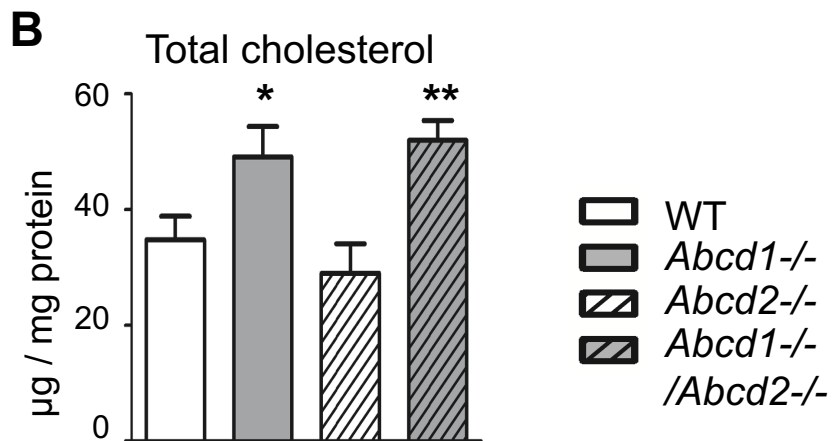
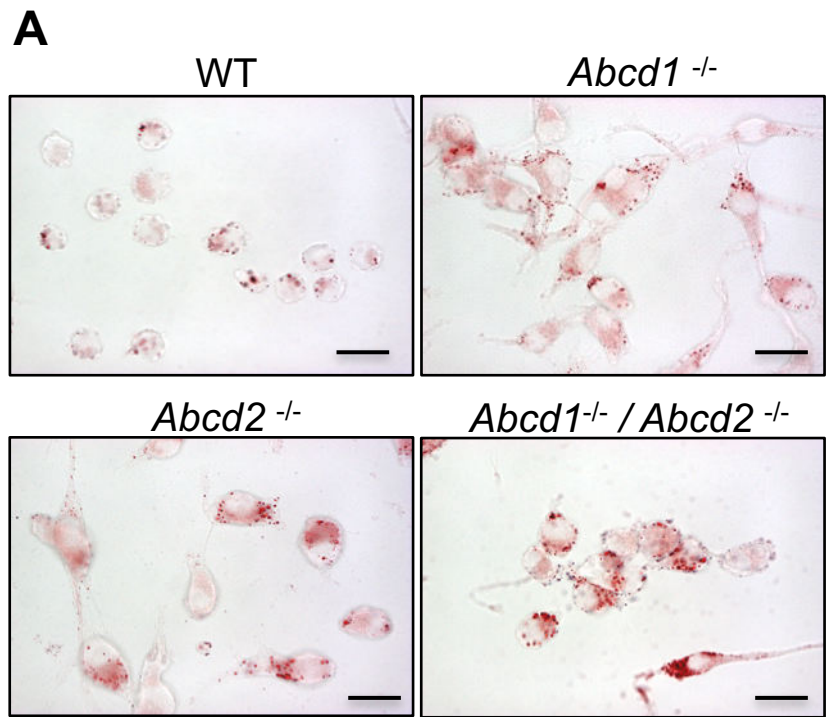


**Fig. 6**



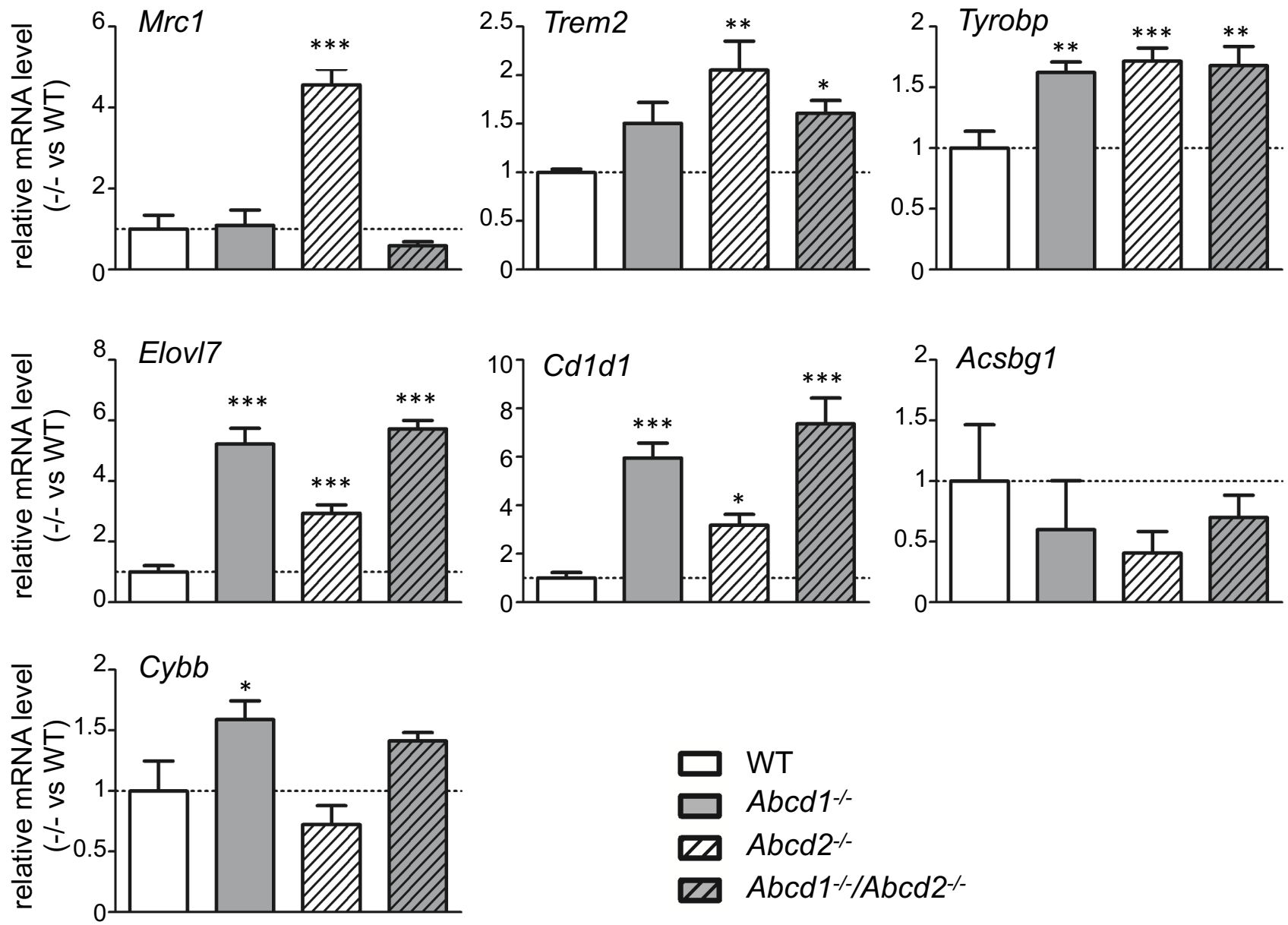


**Fig. 7**